

Magnetic fabric (AMS) of fossil and recent “mud cracks”: Allows to identify an early rock-fabric acquisition during desiccation of unconsolidated sediments?

Fábrica magnética (ASM) de “mud cracks” fósiles y recientes: ¿fábrica temprana adquirida durante la desecación de sedimentos inconsolidados?

Andrés Gil Imaz, Óscar Pueyo Anchuela and Andrés Pocoví Juan

Departamento de Ciencias de la Tierra, Universidad de Zaragoza. C/ Pedro Cerbuna 12, 50009, Zaragoza, España.
agil@unizar.es, opueyo@unizar.es, apocovi@unizar.es

ABSTRACT

In this work the question about the rock-fabric acquisition in mud rocks is analyzed in unconsolidated sediments affected by mud cracks. In this work we study the magnetic fabric (AMS) of three types of fossil and recent mud cracks in order to determine the applicability of this technique to identify the early process involved in the rock-fabric acquisition. The obtained results indicate that the magnetic fabric agrees with a isotropic process similar to a radial contraction. It is emphasized the interest of the AMS technique to investigate the earliest stages of the rock-fabric acquisition.

Key-words: Mud cracks, magnetic fabric, rock-fabric.

RESUMEN

En este trabajo se analiza la adquisición de la petrofábrica en sedimentos inconsolidados afectados por fracturación asociada a desecación (mud cracks). El estudio se desarrolla a partir del análisis de la fábrica magnética (ASM) de tres tipos de mudcracks fósiles y recientes, con el objetivo de determinar la aplicabilidad de la técnica a la hora de identificar procesos físicos tempranos de adquisición de la petrofábrica. Los resultados obtenidos indican que la fábrica magnética es compatible con un proceso físico isótropo similar a una contracción radial. Se pone de manifiesto el interés de la técnica de la ASM en la investigación de los estadios más tempranos de adquisición de la petrofábrica.

Palabras clave: Grietas de desecación, fábrica magnética, petrofábrica.

Geogaceta, 53 (2013), 125-128.
ISSN (versión impresa): 0213-683X
ISSN (Internet): 2173-6545

Fecha de recepción: 9 de julio de 2012
Fecha de revisión: 25 de octubre de 2012
Fecha de aceptación: 30 de noviembre de 2012

Introduction

Cracking of mud sediments or soils during dehydration is an ubiquitous phenomenon commonly observed on drying puddles, river-flood plains and lake margins. Resulting cracks, known as “mud cracks” or “desiccation cracks”, are geometrically characterized by sets of vertical-planar fractures that divide the sediment into prismatic columns similar to those generated at disjunction processes during magma cooling.

The relationship between its geometrical and petrological features and the dynamics of crack opening during drying of stratified sediments, have been extensively described (e.g. Pettijonh, 1957; Allen, 1985; Weinberger, 1999; Vogel *et al.*, 2005; among others).

Two opposite models to explain the nucleation and propagation of mud cracks have been proposed. The classical, and most

accepted model, propose a downward propagating cracks that nucleate at the surface (probably on sediment anisotropies as biogenic imprints, worm tracks or air bubbles), and where the tensile stress is maximum (Neal *et al.*, 1968; Selley, 1982; Allen, 1985). Such pattern is consistent with a downward decrease of both the rate of moisture loss and capillary forces. The downward crack disappearance is consistent with the progressive increase of the horizontal compressive stress linked to the overlaying sediment weight (Allen, 1985).

On the contrary, the second model considers that the mud cracks nucleate at the bottom of the sediments and propagate upward toward the free surface and laterally outward toward adjacent cracks (Weinberger, 1999, 2001). The flaw distribution within the sediment is the main factor controlling the cracks nucleation at depth.

In both cases it is assumed that: 1)

cracks in soils and muds are due to the shrinkage of drying sediment and 2) this physical process gives an isotropic, horizontal, tensional stress field. Independently the mechanism of initiation and growth of the cracks, a limited knowledge about the internal rock-fabric of such structures exists.

In this work, different types of mud cracks linked to different types of soils are analyzed through their magnetic AMS fabric (Anisotropy of magnetic susceptibility). The objective of this work is to analyze if the magnetic fabric can be use to identify the dynamic process of cracks formation.

Experimental method and materials

The anisotropy of magnetic susceptibility (AMS) technique is based on the measurement of the variation of susceptibility in a standard volume of rock when a weak

magnetic field ($\leq 1\text{mT}$) is applied in different directions. Such variation can be described mathematically by means of a second-rank symmetric tensor, which can be physically expressed as an ellipsoid whose principal axes represent the three principal susceptibilities (maximum, intermediate and minimum susceptibility axes, or $K1 \geq K2 \geq K3$).

The preferred orientation of crystallographic axes (crystalline anisotropy) determines the AMS for the majority of minerals (mainly in paramagnetic minerals). In the case of magnetite, the AMS is controlled by the shape preferred orientation of individual grains or grain aggregates (shape anisotropy). In this study we use the P' (corrected anisotropy degree) and T (shape parameter) parameters to characterize the magnitude and shape of the susceptibility ellipsoid (Jelinek, 1981).

The P' parameter is used to quantify the degree of magnetic anisotropy and T characterizes the shape of the AMS ellipsoid. In addition to these parameters, we also use the mean susceptibility parameter $K_m = (K1 + K2 + K3)/3$.

Specimens were measured with a KLY-3s (from Agico), with an operating frequency of 875 Hz and a field intensity of 300 A/m. To identify the magnetic phases present in the samples, curves of the variation of magnetic susceptibility with temperature (susceptibility versus temperature curves or KT curves) were measured in an Ar atmosphere using a CS-3 furnace plugged to the KLY-3s (Hrouda, 1994). Specimens were progressively heated up to 700 °C and subsequently cooled to room temperature. The obtained data from the K/T curves were corrected to avoid device noises (free furnace correction). The variation of susceptibility between room temperature and 200°C was used to analyze the paramagnetic and ferromagnetic contribution to the susceptibility (hyperbolic variation of paramagnetic susceptibility following the Curie-Weiss law).

The studied samples come from three different geological contexts (Fig. 1): 1) Upper Miocene fossil lacustrine mud cracks (Ebro Basin) (site MC01), 2) recent flood-plain mud cracks with a metric-scale size (site MC02); and 3) recent mud cracks formed in an anthropic disposal of fine grain-size detrital material (site MC03). In the first case the samples were obtained "in situ" with a gasoline portable drill. In the

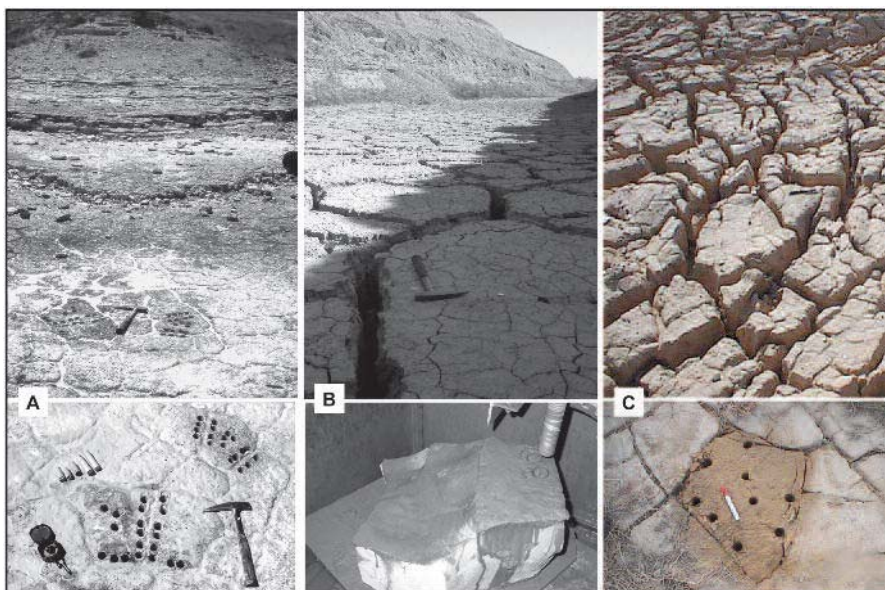


Fig. 1.- Field aspects of the sampled sites. A) Cracks in upper Miocene lacustrine limestones (Ebro Basin, Spain). Site MC01. B) Decimetric-scale mud cracks in recent flood plain marls. Site MC02. C) Cracks in fine grain-size detrital material linked to anthropic disposal. Site MC03.

Fig. 1.- Aspecto de campo de las estaciones analizadas. A) Grietas de desecación en calizas lacustres del Mioceno superior (Cuenca del Ebro, España). Estación MC01. B) Mud cracks decimétricas en margas recientes desarrolladas sobre una llanura de inundación. Estación MC02. C) Grietas de desecación en materiales detríticos de grano fino relacionado con un vertido antrópico. Estación MC03.

second case, two oriented block were drilled in the laboratory. In the third case, and due to the extremely "soft" nature of the sediment, it was employed a specific routine of sampling and manipulation. In the first and second cases, between ten to twelve oriented cores were obtained at each polygon representing 142 and 39 specimens respectively, of 10.3 cm³ in volume. In the soft material of anthropic origin a total of 44 specimens were obtained. In all the cases, samples from both the center and the borders were sampled.

From a petrographic point of view, the lacustrine limestones are composed by a fine-recrystallized micritic carbonate with abundant bioclasts and abundant organic matter linked to bacterial activity (Fig. 2A). In the second case, the sediment constitutes marls with a coarse recrystallized carbonatic matrix and dispersed detrital components. In contrast with the lacustrine limestones, this sediment is characterized by a high content in opaque grains (Fig. 2B).

Results

Magnetic sources

The bulk magnetic susceptibility (K_m ; Table I), show variable results between the analyzed sites. Site MC01 show the lowest

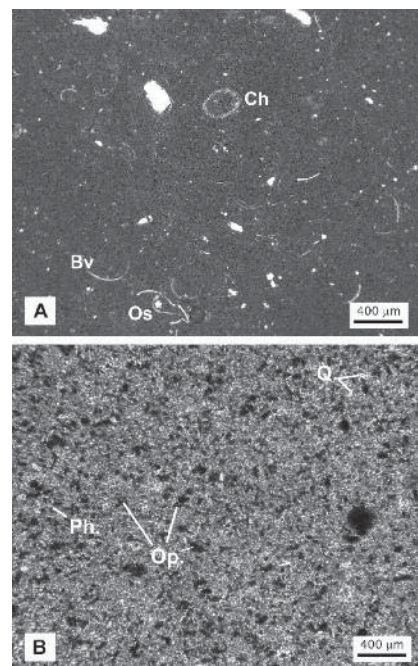


Fig. 2.- A) Microphotograph corresponding to a lacustrine limestone from site MC01. B) Microphotograph corresponding to a marl from site MC02. Ch: characeas, Bv: bivalves, Os: Ostracodes, Q: quartz, Ph: phyllosilicates, Op: opaques.

Fig. 2.- A) Microfotografía de una caliza lacustre de la estación MC01. B) Microfotografía de una marga de la estación MC02. Ch: caráceas. Bn: bivalvos, Os: ostrácodos, Q: cuarzo, Ph: filossilicatos, Op: opacos.

| | Sites | n | Km | P' | T |
|------|--------|----|------------|---------------|--------------|
| MC01 | Center | 44 | 8.7 ± 4 | 1.026 ± 0.02 | 0.389 ± 0.3 |
| | Border | 98 | 7.8 ± 3.5 | 1.027 ± 0.01 | 0.098 ± 0.4 |
| MC02 | Center | 14 | 701.5 ± 56 | 1.041 ± 0.004 | 0.921 ± 0.04 |
| | Border | 25 | 666.6 ± 74 | 1.039 ± 0.004 | 0.890 ± 0.06 |
| MC03 | Center | 13 | 261.2 ± 20 | 1.013 ± 0.003 | 0.475 ± 0.4 |
| | Border | 31 | 241.7 ± 31 | 1.017 ± 0.007 | 0.560 ± 0.3 |

Table I.- Site mean anisotropy susceptibility data for the analyzed samples. n: number of analyzed specimens, Km: mean susceptibility (x 10⁻⁶ SI units), P' = degree of anisotropy and T: shape parameter. (Jelinek, 1981).

Tabla I.- Datos medios por estación de las muestras analizadas. n: número de especímenes analizados, Km: susceptibilidad media (x 10⁻⁶ unidades SI), P': grado de anisotropía, y T: parámetro de forma. (Jelinek, 1981).

values with a mean value of 8.0 x 10⁻⁶ SI. On the contrary, site MC02, show the highest Km values with an average bulk susceptibility of 677 x 10⁻⁶ SI. In this case these values agree with the high content in opaque grains (ferromagnetic phases) identified in the microphotographs. Although high differences between the mean bulk Km values for the different sites occurs, it is not significant between the border and the central samples.

On the other hand, excepting the inverse relationship between the whole-rock degree of anisotropy (P') and the mean bulk susceptibility (Km) found in site MC01 probably linked to its diamagnetic behaviour, no positive correlation between both parameters exists (Fig. 3A). This fact indicates that the degree of AMS anisotropy in the rock-specimens is independent from the mineral content.

The KT curves show different rates of ferromagnetic contributions to the susceptibility (Fig. 3B). At this sense for sites MC01 and MC03, ferromagnetic contribution can be estimated in 23% and near to 50% respectively. On the other hand, the observed increase of the susceptibility in the RT-200°C part of the heating curve MC02, probably indicate the creation of new minerals during heating or the unblocking of superparamagnetic grains.

Magnetic fabric

Site MC01 show a high dispersion for both the ellipsoid shapes (T) (especially for specimens coming from the borders) and for the degree of anisotropy (P') (Fig. 4). On the contrary, a very high cluster of T values, close to T=1 (pure oblate uniaxial ellipsoids) is observed in site MC02. Site MC03 show an intermediate dispersion pattern of ellip-

soid shapes for samples coming from both the center and border. Independently of the differences between sites, the pattern distribution for the P' and T parameters is quite similar for each single site irrespective of the samples location (center/border).

Concerning the directional analysis, in all the cases the orientation of the different axes does not differ between center to border location of the studied samples (Fig. 5).

Maximum and intermediate susceptibility axes display a radial pattern without a well defined magnetic lineation. On the contrary, the Kmin axes are well grouped in a vertical location. In the case of site MC03 a slight tilting for the magnetic foliation (plane containing the Kint. and Kmax axes) is identified in the same manner than the topographical surface. The directional patterns for each site agrees with the distribution pattern observed in the anisotropy plots (Fig. 4). The most uniaxial and highest T values are identified at the MC02 site.

Discussion: Does AMS fabric reveals the cracking process?

The rock-fabric acquisition related to cracking formation represents a singular case of an early fabric related with different geometric and dynamic aspects of the crack surfaces (Neal *et al.*, 1968; Allen, 1985; Vogel *et al.*, 2005; among others).

The characterization and identification of earliest stages of the rock-fabric acquisition has been a long-standing debate. In the case of tractive streams, flow energy is the main responsible of the rock-fabric with shallowly sloping depositional surfaces and particle arrangement due to the flow current. In the case of muddy sediments, are Brownian forces and clay agglomerates flocculation the main processes controlling

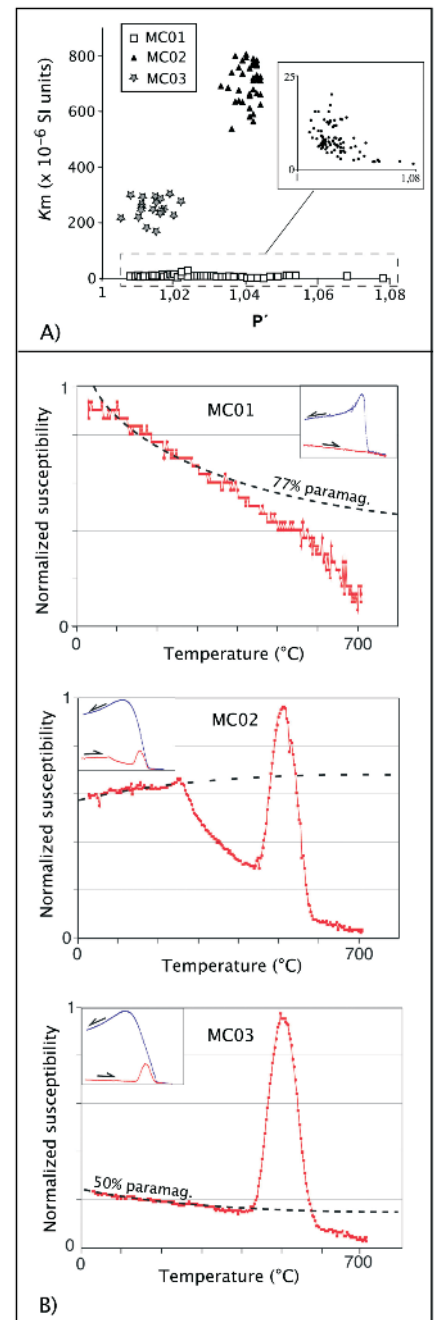


Fig. 3.- A) Km versus P' plot for the analyzed samples. B) Representative temperature-dependent magnetic susceptibility curves (KT curves) from the studied sites and paramagnetic contribution calculation.

Fig. 3.- A) Gráfico Km vs. P'. B) Curvas representativas de variación de la susceptibilidad media (Km) con la temperatura (T) (curvas KT), de las estaciones analizadas y cálculo de la contribución paramagnética.

the rock-fabric acquisition resulting in an isotropic fabric (Osipov and Sokolov, 1978).

From preliminary results of the AMS analysis in fossil and recent "mud cracks", some considerations about the origin of their rock-fabric acquisition can be made. Firstly, a clear magnetic lineation is not

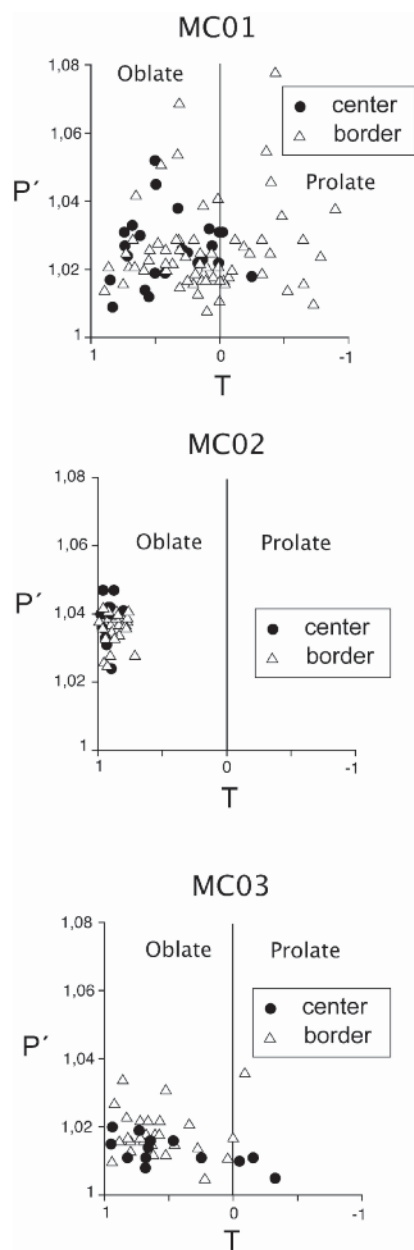


Fig. 4.- Anisotropy plots for the center/border analyzed samples from the studied cracks. P': degree of anisotropy, T: shape parameter.

Fig. 4.- Gráfico de anisotropía para las muestras del centro y borde de las tres mud-cracks analizadas. P': grado de anisotropía, T: parámetro de forma.

found from the magnetic fabric, suggesting a scarce (or very weakly) effect of tractive

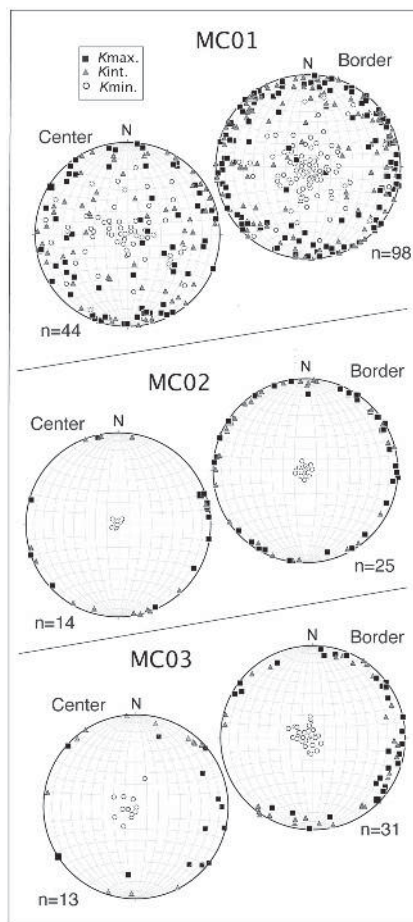


Fig. 5.- Equal-area projections of the principal susceptibility axes for the border/center analyzed samples from the studied cracks.

Fig. 5.- Proyecciones estereográficas de los ejes principales de susceptibilidad para las muestras analizadas del centro y borde de las mud-cracks estudiadas.

streams. On the other hand, the marked anisotropic behaviour of the magnetic fabric (predominance of oblate-uniaxial ellipsoids) and the conspicuous radial directional pattern (Kmax and Kint axes scattered around the horizontal plane), with independence of the samples location (center/border) (Figs. 4 and 5), agrees with a physical isotropic process like a radial tensile stress field controlled by the own crack geometry.

The maximum dispersion for both the magnetic parameters (P' and T) and magnetic directions is found for the Upper Miocene lacustrine (site MC01) where evidences of bioturbation exists.

These preliminary results suggest that the magnetic fabric in soft sediments can be more sensible to an early isotropic diagenetic process than to one more anisotropic sedimentary one (imbrication, rolling, flow current...). The obtained results emphasize the possibilities of the AMS technique in order to investigate the earliest stages of the rock-fabric acquisition.

Acknowledgements

This paper is supported by funds of the GEOTRANSFER research group. We acknowledge the constructive review and comments by Juanjo Villalaín and an anonymous reviewer, which helped to improve the original manuscript.

References

Allen, J.R.L. (1985). *Principles of Physical Sedimentology*. George Allen and Unwin, London, 272 p.
 Hrouda, F. (1994). *Geophysical Journal Interiors*, 118, 604-612.
 Jelinek, V. (1981). *Tectonophysics*, 70, 63-67.
 Neal, J.T., Langer, A.M. and Keer, P.F. (1968). *Geological Society of America, Bulletin*, 79, 69-90.
 Osipov, V.I. and Sokolov, V.N. (1978). In: *Scanning electron microscope in the study of sediments* (W.B. Whalley, Ed.). Geo Abstracts, Norwich, England, 29-40.
 Pettijohn, F.J. (1957). *Sedimentary Rocks*. Harper and Brothers. New York, 718 p.
 Selley, R.C. (1982). *An Introduction to Sedimentology*. Academic Press, New York, 408 p.
 Vogel, H.J., Hoffmann, H., Leopold, A. and Roth, K. (2005). *Geoderma*, 125, 213-223.
 Weinberger, R. (1999). *Journal of Structural Geology*, 21, 379-386.
 Weinberger, R. (2001). *Geological Society of America Bulletin*, 113, 20-31.